Published December 31, 2007

Mice deficient in involucrin, envoplakin, and periplakin have a defective epidermal barrier

Lisa M. Sevilla,[1] Rachida Nachat,[1] Karen R. Groot,[2] John F. Klement,[3] Jouni Uitto,[3] Philippe Djian,[4] Arto Määttä,[5] and Fiona M. Watt[1,6]

[1]Cancer Research UK, Cambridge Research Institute, Li Ka Shing Centre, Cambridge CB2 0RE, England, UK
[2]National Cancer Research Institute, London WC2A 3PX, England, UK
[3]Department of Dermatology and Cutaneous Biology, Thomas Jefferson University, Philadelphia, PA 19107
[4]Unité Propre de Recherche 2228, Centre National de la Recherche Scientifique, Institut Interdisciplinaire des Sciences du Vivant des Saints-Peres, Université Rene Descartes, 75006 Paris, France
[5]School of Biological and Biomedical Sciences, University of Durham, Durham DH1 3LE, England, UK
[6]Wellcome Trust Centre for Stem Cell Research, Cambridge CB2 1QR, England, UK

The cornified envelope is assembled from transglutaminase cross-linked proteins and lipids in the outermost epidermal layers and is essential for skin barrier function. Involucrin, envoplakin, and periplakin form the protein scaffold on which the envelope assembles. To examine their combined function, we generated mice deficient in all three genes. The triple knockouts have delayed embryonic barrier formation and postnatal hyperkeratosis (abnormal accumulation of cornified cells) resulting from impaired desquamation. Cornified envelopes form but are ultrastructurally abnormal, with reduced lipid content and decreased mechanical integrity. Expression of proteases is reduced and the protease inhibitor, serpina1b, is highly upregulated, resulting in defective filaggrin processing and delayed degradation of desmoglein 1 and corneodesmosin. There is infiltration of $CD4^+$ T cells and a reduction in resident $\gamma\delta^+$ T cells, reminiscent of atopic dermatitis. Thus, combined loss of the cornified envelope proteins not only impairs the epidermal barrier, but also changes the composition of T cell subpopulations in the skin.

Introduction

The outermost, cornified, layers of the epidermis are composed of terminally differentiated keratinocytes known as corneocytes. Corneocytes lack a plasma membrane and instead are encased in a structure known as the cornified envelope (CE) (Rice and Green, 1977). CEs consist of highly insoluble, cross-linked proteins with covalently attached lipids and are essential for the mechanical integrity and water impermeability of the skin (Candi et al., 2005; Segre, 2006).

CE assembly is triggered in differentiating keratinocytes by a rise in intracellular Ca^{2+}, which activates the membrane-associated transglutaminase 1 enzyme. Transglutaminase 1 catalyzes both the formation of N^{ε}-(γ-glutamyl)lysine cross-links between CE precursor proteins and the attachment of long chain ω-hydroxyceramides via ester linkages onto glutamine residues (Marekov and Steinert, 1998; Nemes et al., 1999). The covalently bound lipids replace the plasma membrane and are hypothesized to direct the organization of specialized lipids, secreted from differentiating keratinocytes, into ordered lipid lamellae that fill the intercellular space between corneocytes (Kalinin et al., 2002). The importance of protein–protein and protein–lipid cross-linking in the epidermis is underscored by the phenotype of mice lacking transglutaminase 1, which die shortly after birth due to transepidermal water loss (Matsuki et al., 1998).

The three proteins that are first incorporated into the CE are involucrin, envoplakin, and periplakin (Rice and Green, 1979; Simon and Green, 1984; Ruhrberg et al., 1996, 1997). The *involucrin* locus resides within the epidermal differentiation complex (human chromosome 1q21, mouse 3F2.1), a cluster of more than 30 genes expressed late in terminal differentiation. Involucrin becomes cross-linked to almost all other CE proteins and is the principal substrate for transglutaminase 1–mediated attachment of ω-hydroxyceramides (Marekov and Steinert, 1998).

Envoplakin and periplakin belong to the plakin protein family and are encoded by genes outside of the epidermal differentiation complex (Jefferson et al., 2004). They form stable heterodimers that localize to desmosomes and the plasma

L.M. Sevilla and R. Nachat contributed equally to this paper.

Correspondence to Fiona M. Watt: fiona.watt@cancer.org.uk

Abbreviations used in this paper: CE, cornified envelope; E, embryonic day; HET, heterozygous; KO, knockout; P, postnatal day; WT, wild type.

The online version of this article contains supplemental material.

Supplemental Material can be found at:
http://jcb.rupress.org/content/suppl/2008/02/01/jcb.200706187.DC1.html

The Journal of Cell Biology, Vol. 179, No. 7, December 31, 2007 1599–1612
http://www.jcb.org/cgi/doi/10.1083/jcb.200706187

Published December 31, 2007

membrane in a manner dependent on the periplakin N terminus (DiColandrea et al., 2000). Kazrin, a recently identified periplakin binding partner, may play a role in directing periplakin to the membrane (Groot et al., 2004). The C termini of envoplakin and periplakin bind intermediate filaments, and it is likely that the link they provide between the cytoskeleton and the CE confers mechanical stability to corneocytes (Karashima and Watt, 2002; Kazerounian et al., 2002).

Immunogold electron microscopy and amino acid sequencing of peptides isolated from CEs indicate that the earliest cross-linking events during CE assembly are between involucrin and envoplakin at the interdesmosomal plasma membrane (Steinert and Marekov, 1999). Thus, involucrin, envoplakin, and periplakin form a scaffold spanning the inner surface of the plasma membrane and the desmosomes, onto which proteins and lipids assemble to form the mature CE (Robinson et al., 1997; Steinert and Marekov, 1999).

The normal physiology of the skin requires both the proper formation and the controlled shedding (desquamation) of the cornified layers. The integrity of the cornified layers depends on modified desmosomes known as corneodesmosomes (Skerrow et al., 1989; Serre et al., 1991). These form at the granular layer/stratum corneum interface when preexisting desmosomes lose their cytoplasmic plaque, which becomes fully incorporated into the CE. In addition to the transmembrane components of granular layer desmosomes, desmoglein 1 and desmocollin 1, corneodesmosomes contain an extracellular protein known as corneodesmosin (Serre et al., 1991; Simon et al., 1997). Desquamation depends on the proteolytic degradation of corneodesmosome proteins (Guerrin et al., 1998; Simon et al., 2001). Decreased epidermal protease activity can contribute to the corneodesmosome retention observed in some forms of ichthyoses, disorders that are characterized by a scaly appearance of the skin as a result of hyperkeratosis or thickening of the stratum corneum (Ghadially et al., 1992; Elias et al., 2004; Basel-Vanagaite et al., 2007).

Despite the near-ubiquitous presence of involucrin, envoplakin, and periplakin in CEs of stratified squamous epithelia, loss of expression of any one of the proteins does not significantly compromise barrier function in mice: the animals are viable, fertile, and do not have obvious skin abnormalities (Djian et al., 2000; Määttä et al., 2001; Aho et al., 2004). Similarly, mice deficient in loricrin, which comprises ~80% of CE protein mass, have only a subtle phenotype, with transient, mild epidermal erythema and increased CE fragility (Koch et al., 2000). These studies indicate that although assembly of the CE is essential for skin function, the precise protein composition of the envelope is less important and suggest the existence of strong compensatory mechanisms for loss of individual CE proteins. To examine this, we generated mice triply deficient in involucrin, envoplakin, and periplakin.

Results

Generation of triple knockout mice

The genotype of the *envoplakin*$^{-/-}$*;involucrin*$^{-/-}$*;periplakin*$^{-/-}$ (triple knockout) mice was assessed by Southern blotting (Fig. S1 A, available at http://www.jcb.org/cgi/content/full/jcb.200706187/DC1). The lack of expression of the CE scaffold proteins was confirmed by immunostaining sections of E17.5 dorsal skin isolated from triple knockout (KO) or triple heterozygous (HET) mice with antibodies specific for envoplakin, involucrin, or periplakin (Fig. S1 B).

All double KO combinations generated as intermediates during the breeding of the triple KOs, *envoplakin*$^{-/-}$*;involucrin*$^{-/-}$, *envoplakin*$^{-/-}$*;periplakin*$^{-/-}$, and *involucrin*$^{-/-}$*;periplakin*$^{-/-}$, were viable, fertile, and had no overt phenotypic abnormalities. We predicted that combined loss of the three proteins would result in a more severe CE phenotype; however, remarkably, the triple KO mice were viable.

Triple KO mice develop dry, ichthyosiform skin

Immediately after birth, triple KO mice were indistinguishable from the age-matched wild-type (WT) or triple HET controls, showing neither overt skin abnormalities nor size differences from ages P0 to P3/P4 (unpublished data). The histology of the living cell layers of the P1 triple KO epidermis was similar to that of WT. However, the triple KO stratum corneum was significantly more dense than that of WT (Fig. 1 A), especially in the lower layers adjacent to the granular layer. By day P4/P5, a striking phenotype of dry, flaky skin was apparent and scales were present over the entire surface of triple KO mice, particularly on the dorsal side (Fig. 1 B).

Histological analysis of the affected skin revealed hyperkeratosis (Fig. 1 C). This did not correlate with an increase in the number of viable cell layers or an increase in cell proliferation (Fig. 1 C; unpublished data). Parakeratosis, retention of nuclei in the cornified layers, was rare in the triple KO epidermis, consistent with the normal appearance of the granular layer (Fig. 1 C). After the first anagen stage, the hyperkeratotic scales were no longer evident on gross inspection (unpublished data), possibly due to the added barrier protection provided by hair. However, hyperkeratosis persisted in adult triple KO mice (Fig. 1 D). Hyperkeratosis was not observed in the epidermis of adult envoplakin, involucrin, or periplakin single KO mice (Fig. S2 A, available at http://www.jcb.org/cgi/content/full/jcb.200706187/DC1). Overall, these data suggest defects in the late stages of terminal differentiation and in desquamation that are unique to triple KO mice.

Triple KO mice exhibit a delay in permeability barrier acquisition

Although the triple KO mice had a functional permeability barrier after birth, it was possible that in utero, acquisition of the barrier was impaired. To test this, WT, triple HET, and triple KO embryos were collected at embryonic days E16.5 and E17.5, the period when patterned acquisition of the permeability barrier occurs (Hardman et al., 1998), and subjected to the toluidine blue dye penetration assay. While at day E16.5, triple HET embryos (Fig. 1 E, red arrows) had dorsal dye-excluding regions, evidence of barrier initiation, triple KO embryos were entirely dye permeable (Fig. 1 E). At day E17.5, both WT and triple HET embryos had nearly intact permeability barriers, while the

Published December 31, 2007

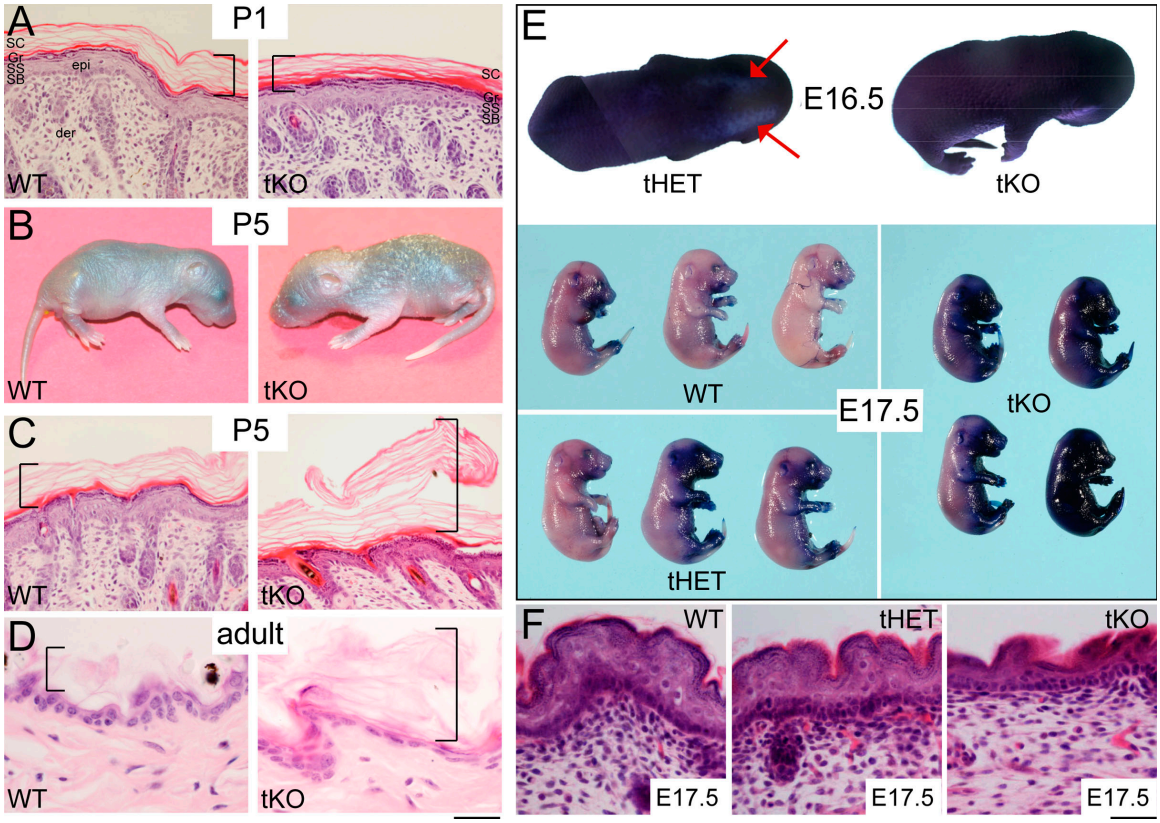

Figure 1. **Triple KO mice exhibit hyperkeratosis and a delay in embryonic barrier formation.** (A) Histology of newborn P1 dorsal skin. Epi, epidermis; der, dermis; SB, stratum basale; SS, stratum spinosum; Gr, stratum granulosum; SC, stratum corneum; tKO, triple KO. Brackets (A, C, and D) indicate cornified layers. Bar: 100 μm. (B) P5 triple KO mice exhibit dry, scaly skin relative to WT. (C) Histology of P5 triple KO skin indicates hyperkeratosis relative to WT. Bar: 100 μm. (D) Histology of adult WT and triple KO dorsal skin. Bar: 50 μm. (E) Toluidine blue dye exclusion assay with E16.5 (top panel) and E17.5 (bottom panels) WT, triple HET, and triple KO embryos. Red arrows indicate barrier initiation sites in E16.5 triple HET embryo. (F) Histology of E17.5 WT, triple HET, and triple KO dorsal skin. Bar: 50 μm.

epidermis of the triple KO embryos was still mostly dye permeable, evidence for a delay in barrier acquisition (Fig. 1 E). Histological analysis of E17.5 dorsal skin indicated that the triple KO epidermis was thinner than that of WT or triple HET (Fig. 1 F), suggesting an overall delay in its development.

Ultrastructural changes in the desmosomes and stratum corneum of triple KO epidermis

We examined the ultrastructure of adult triple KO epidermis by transmission electron microscopy (Fig. 2). The overall morphology of the living cell layers in the triple KO epidermis appeared similar to that of the *involucrin*$^{+/-}$ control (Fig. 2 A). However, detailed inspection revealed several differences. The desmosomal plaques in the triple KO epidermis had a decreased electron density relative to those of the control (Fig. 2 B, black arrows), consistent with envoplakin and periplakin being plaque components. In the first corneocyte layer of normal stratum corneum, a peripheral electron-dense line can be observed that is indicative of a mature CE (Fig. 2 C, asterisk). The electron density of this line was markedly reduced in the triple KO (Fig. 2 C, asterisk), suggestive of altered CE composition and/or maturity. In addition, the corneodesmosomes of the triple KO stratum corneum appeared disorganized (Fig. 2 C, arrows), indicating a defect in the late stages of terminal differentiation. In normal epidermis, corneodesmosomes are degraded in the lower stratum corneum, but in triple KO epidermis corneodesmosomes were present even in the outermost corneocyte layers, a sign of defective desquamation (Fig. 2 C, arrows).

Immunostaining for components of intercellular junctions and differentiation markers in triple KO epidermis

We used immunofluorescence microscopy to investigate whether components of cell junctions and terminal differentiation markers were disturbed in the triple KO mice. Immunostaining with antibodies specific for desmoplakin, E-cadherin, and occludin, components of desmosomes, adherens junctions, and tight junctions, respectively, indicated a normal distribution in triple KO epidermis (Fig. 3 A).

There were no differences observed in α6 integrin or keratin 14 expression in triple KO epidermis (Fig. 3 B; unpublished data). Keratin 1 and 10 were expressed normally in the spinous layer of triple KO epidermis (Fig. 3 B). However, while the epitopes recognized by the keratin 1 antiserum were lost in the upper layers of WT epidermis, they were present in the triple KO (Fig. 3 B). Immunostaining for loricrin, a CE structural protein, demonstrated normal granular layer expression in the

Published December 31, 2007

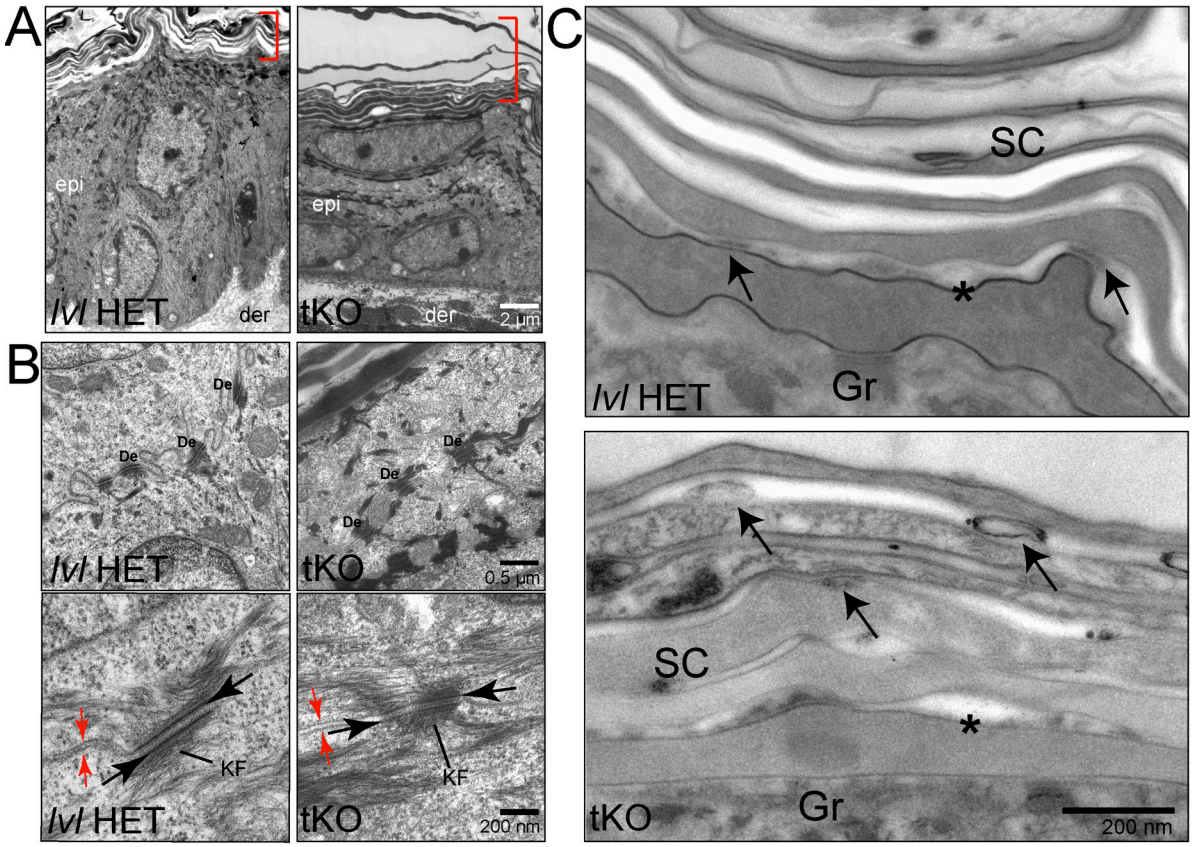

Figure 2. **Ultrastructural changes in triple KO adult epidermis.** (A) Low magnification views of sections of adult control (*involucrin* (*lvl*) HET) and triple KO (tKO) dorsal epidermis. Red brackets mark cornified layers. Epi, epidermis; der, dermis. (B) Higher magnification images of desmosomes (De) and associated keratin intermediate filaments (KF). Triple KO desmosomes have a less distinct plaque (black arrows). Red arrows indicate adjacent cell membranes. (C) Higher magnification images of the granular layer (Gr)-stratum corneum (SC) interface and lower stratum corneum. Note altered morphology and prolonged retention of corneodesmosomes (black arrows) in the triple KO relative to the control. The CE is apparent as an electron dense line at the periphery of the corneocyte adjacent to the granular layer (asterisks). Note the decrease in electron density of this line in the triple KO.

triple KO (Fig. 3 B), consistent with the normal ultrastructural appearance of the granular layer (see below).

Reduced interfollicular epidermal lipids and increased cornified envelope fragility in triple KO mice

Epidermal lipids are critical for a functional barrier and are released from lamellar bodies produced by granular layer keratinocytes as well as from sebaceous glands. There were no obvious differences in the presence and ultrastructure of lamellar bodies observed by electron microscopy (Fig. 4 A, black arrows). In addition, we observed normal extrusion of the lipid contents of the lamellar bodies in triple KO epidermis (Fig. 4 A, white arrows). However, there was an altered organization of the extracellular lipid layers in the triple KO stratum corneum, indicating abnormalities in lipid attachment to CEs (Fig. 4 A, asterisks). Staining of frozen sections of dorsal skin from E17.5 epidermis with Nile Red (a lipophilic dye) showed a dramatic decrease in stratum corneum lipids in the triple KO relative to WT (Fig. 4 B). Similar results were obtained with P5 and adult triple KO epidermis (unpublished data; Fig. S2 B). No decrease in epidermal lipids was detected in adult epidermis from single KO mice (Fig. S2 B), indicating that the decrease in the triple KO mice was due to the combined loss of all three CE scaffold proteins.

Examination of adult tail epidermis using the whole-mount labeling technique revealed that even though the sebaceous glands of the triple KO were slightly enlarged compared with WT controls (Fig. 4 B, brackets), they stained strongly with Nile Red, indicating that lipid production was unaffected (Braun et al., 2003). These results suggested that the reduction in lipids in the triple KO stratum corneum was due to the loss of substrates for lipid attachment rather than to a defect in lipid biosynthesis.

The reduced electron density of the CE in the first corneocyte layer suggested that the absence of involucrin, envoplakin, and periplakin might result in less mechanically resilient CEs (Fig. 2 C). CE sensitivity to mechanical stress was determined by subjecting WT or triple KO CEs to sonication for 0, 30, or 60 s (Koch et al., 2000). Strikingly, while 90% of WT CEs were intact after 30 s of sonication, only 30% of triple KO CEs remained (Fig. 4, C and D). This result demonstrates that triple KO CEs have reduced ability to withstand mechanical stress.

Triple KO epidermis has decreased protease activity

Our analysis demonstrated that in the absence of involucrin, envoplakin, and periplakin, the epidermal barrier was abnormal, and suggested that the compensatory mechanism allowing barrier function to be maintained was reduced desquamation.

Published December 31, 2007

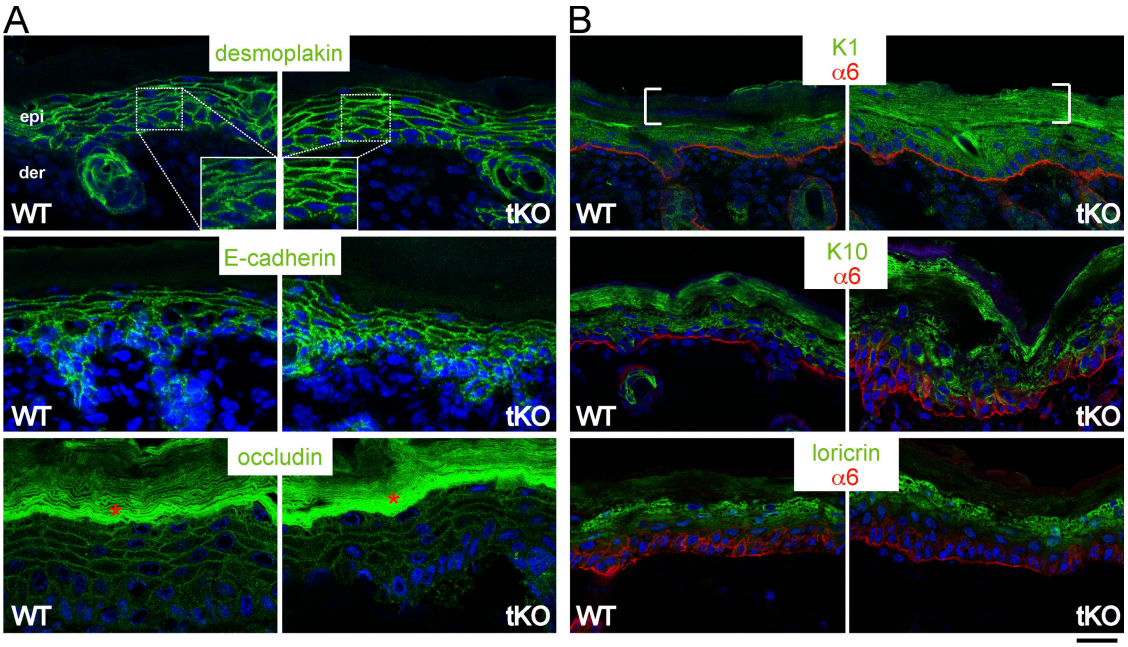

Figure 3. **Analysis of intercellular junctions and differentiation markers in triple KO epidermis.** (A) Immunofluorescence staining of sections of P5 skin with antibodies specific for the following junctional proteins (green): desmoplakin, E-cadherin and occludin. Insets are magnified views of boxed areas. Nuclei are visualized with DAPI (blue). Red asterisks mark unspecific secondary antibody staining of cornified layer. Epi, epidermis; der, dermis. Bar: 20 μm. (B) Immunofluorescence staining of sections of P5 skin with antibodies specific for the following markers of epidermal differentiation (green): keratin 1, keratin 10, and loricrin. Note staining of keratin 1 in cornified layers (brackets) of triple KO epidermis. Antibodies specific for α6 integrin (red) mark the basal layer. Note that depending on the angle at which the section was cut, this staining can appear to extend above the basal layer. Nuclei are visualized with DAPI (blue). Bar: 50 μm.

To investigate how this was achieved, microarray analysis was performed using mRNA isolated from dorsal skin of 7-wk-old WT, triple HET, or triple KO female mice (Fig. 5). Skin histology proximal to that used for RNA isolation indicated hyperkeratosis in the triple KO, but not the WT or triple HET (unpublished data). Consistent with their phenotypes, the triple HET samples clustered more closely with those of WT than with triple KO (Fig. 5 A). 207 genes were found to have statistically significant ($P < 0.05$) changes (twofold or greater; increase or decrease) in expression between WT and triple KO samples (Table S1, available at http://www.jcb.org/cgi/content/full/jcb.200706187/DC1).

Surprisingly, very few genes on the list encoded protein components of the cytoskeleton, adhesive junctions, or CE (Fig. 5 B), indicating minimal compensation at this level. *Lce1d*, a member of the late cornified envelope (LCE) gene family (Marshall et al., 2001; Brown et al., 2007), was the only CE gene identified (2.331-fold greater in triple KO). There were no statistically significant changes in gene expression of transglutaminase enzymes, enzymes involved in CE lipid metabolism, desmosome components, or in other CE structural proteins, including small proline-rich proteins and loricrin.

Two striking features of the microarray were evident. First, a fifth of the genes with altered expression in the triple KO were associated with immune response (Fig. 5 B). Second, expression of genes encoding proteases and protease inhibitors was altered. *Serpin a1b*, which encodes a serine protease inhibitor, was strongly up-regulated (22.89-fold greater in triple KO) (Table S1). Conversely, expression of several proteases was down-regulated, including the cysteine proteases *cathepsin C* (0.422-fold) and *cathepsin S* (0.373-fold), and the serine protease *proteinase 3* (0.494-fold) (Table S1).

The changes in expression of *serpin a1b* and the proteases were confirmed by semi-quantitative RT-PCR using RNA isolated from mouse skin (Fig. 5 C). The change in *serpin a1b* expression was intrinsic to keratinocytes, as *serpin a1b* was also up-regulated in cultured keratinocytes isolated from triple KO mice (unpublished data).

To examine whether the altered expression of the proteases and *serpin a1b* resulted in an overall decrease in epidermal proteolytic activity in the triple KO, we performed in situ zymography on sections of P5 dorsal skin (Fig. 5 D). In this assay, protease activity results in the generation of a fluorescent signal, an effect reduced by addition of the serine protease inhibitor aprotinin. The fluorescence signal intensity was decreased in the triple KO epidermis relative to WT (Fig. 5 D), supporting the prediction from the microarray analysis. The decrease in epidermal protease activity would provide an explanation for the retention of keratin 1 immunoreactivity in the stratum corneum (Fig. 3 B) because the antibody used recognizes a C-terminal epitope that is thought to be cleaved by stratum corneum proteases (Roop et al., 1984).

Epidermal protease activity was also decreased in adult triple KO mice (Fig. S3 A, available at http://www.jcb.org/cgi/content/full/jcb.200706187/DC1). Quantitation of fluorescence intensity in the stratum corneum revealed that adult involucrin single KO mice had a slight decrease in proteolytic activity compared with WT, but that it was not as pronounced as in the triple KO.

Published December 31, 2007

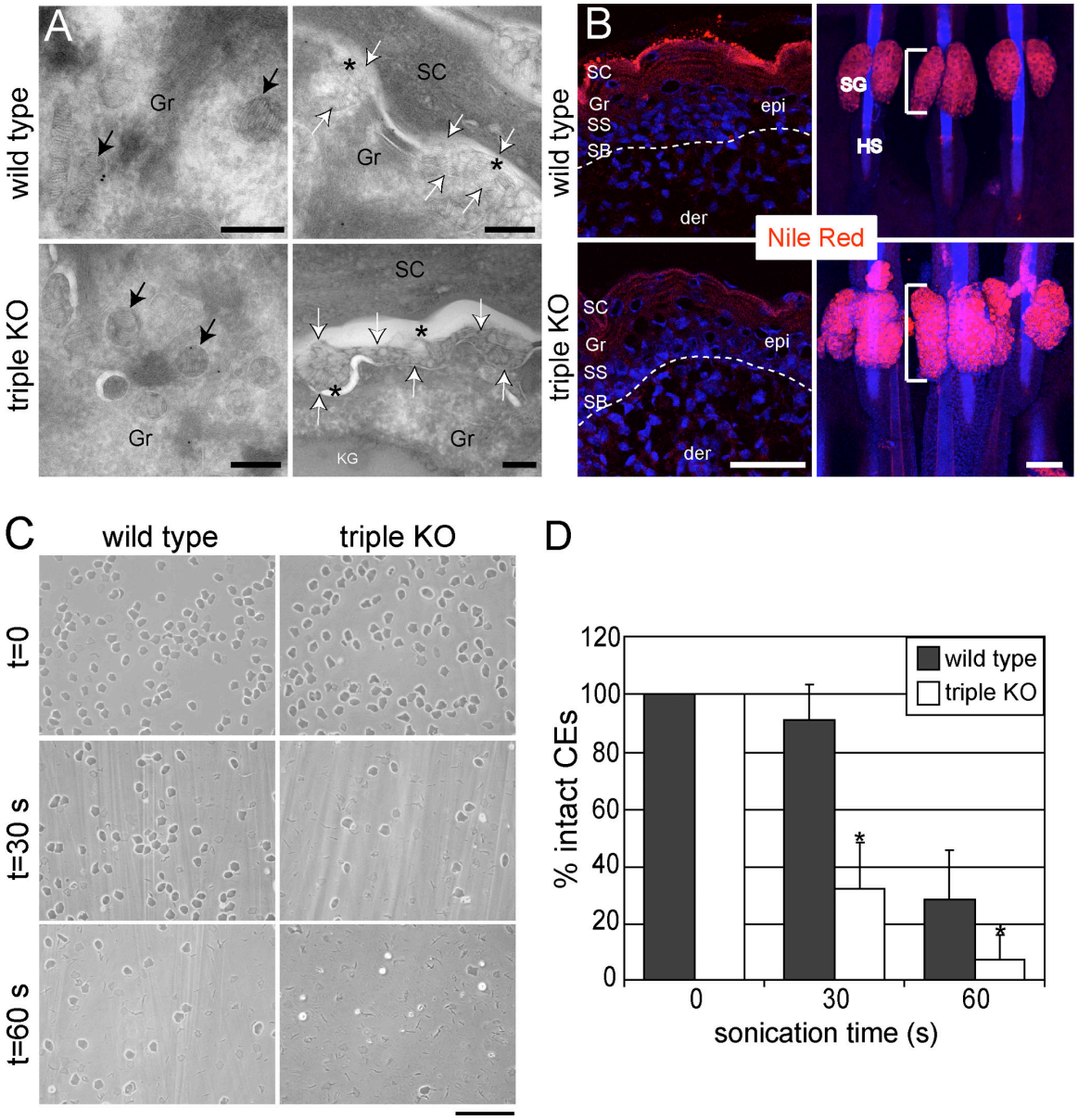

Figure 4. **Two barrier components are affected in triple KOs: CEs and lipids.** (A) Morphological analysis by transmission electron microscopy of lamellar bodies (black arrows) and secreted lamellar lipids (white arrows). Note abnormal attachment of secreted lipids in the triple KO relative to WT (asterisks). Bars: 200 nm. (B) Nile Red staining shows reduced lipid content of cornified layers in E17.5 triple KO epidermis and enlarged sebaceous glands (SG) in whole mounts of adult triple KO tail epidermis (brackets). Broken lines mark the epidermal-dermal border. HS, hair shaft. Bars: 50 μm. (C) Representative micrographs of WT or triple KO CEs, which were either untreated (t = 0) or subjected to sonication for 30 (t = 30) or 60 (t = 60) seconds. Bar: 200 μm. (D) Following sonication, intact envelopes were counted with a hemocytometer. Data are presented as the averages of CE preparations from three mice per genotype with at least two independent sonication experiments performed per preparation (+ standard deviation). Asterisk indicates a two-tailed P value <0.02, by paired *t* test ($n = 7$ per genotype).

There was no reduction in epidermal protease activity in envoplakin and periplakin single KO mice (Fig. S3 A).

Decreased protease activity in triple KO epidermis affects the degradation of desmoglein 1/2 and corneodesmosin, and the processing of profilaggrin

The hyperkeratosis (Fig. 1) and corneodesmosome retention (Fig. 2 C) in triple KO epidermis suggested that reduced epidermal proteolysis results in a defect in degradation of corneodesmosome proteins. The immunofluorescence signal intensity for desmoglein 1/2 in the living cell layers of the triple KO epidermis was similar to that of WT (Fig. 6 A). However, as the desmoglein 1/2 antibody epitope is masked in the granular layer due to a Ca^{2+}-dependent conformational change (Amagai et al., 1995), its levels were further analyzed by immunoblotting insoluble protein extracts from adult dorsal skin. There was an increase in the intensity of the band corresponding to desmoglein 1/2 in the triple KO relative to triple HET and WT samples, consistent with reduced degradation in the outer epidermal layers (Fig. 6 B). Immunofluorescence microscopy indicated that the corneodesmosin epitope was maintained in the upper

Published December 31, 2007

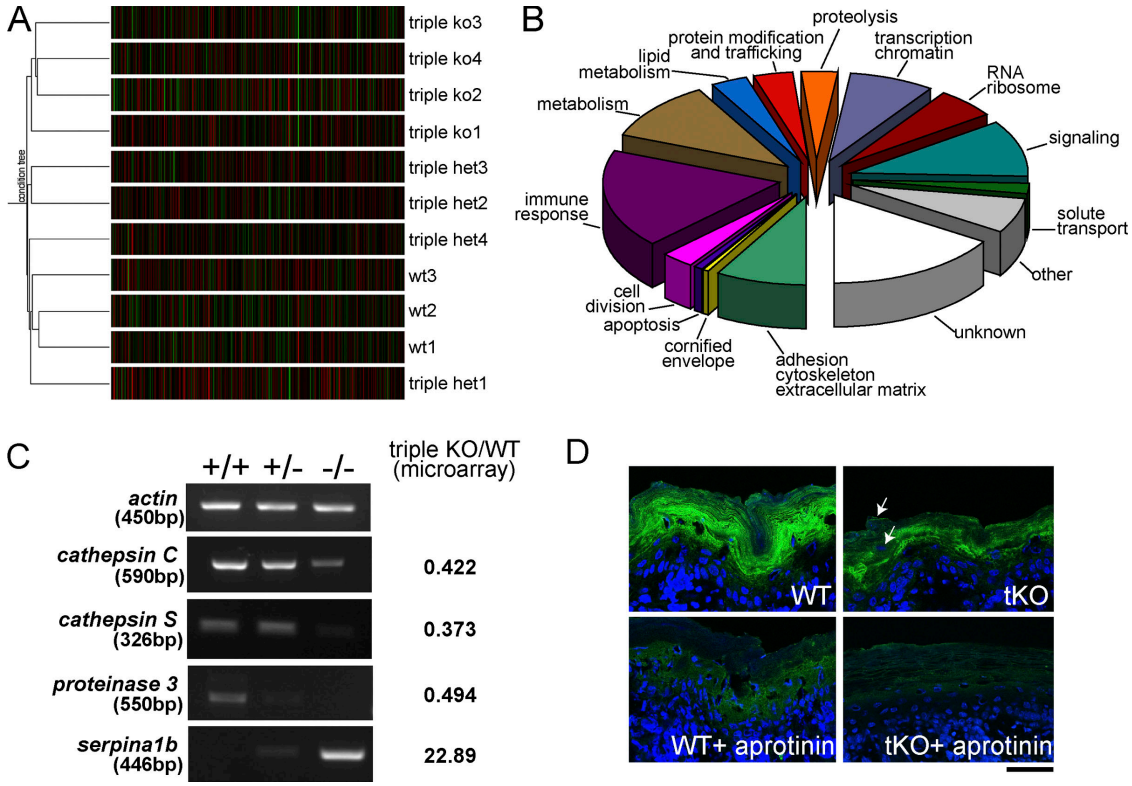

Figure 5. **Microarray analysis reveals changes in epidermal protease activity.** (A) Clustering of microarray data. Note that triple HET samples cluster more closely with WT than with triple KO. (B) Pie graph of genes (grouped according to function) with altered expression in triple KO relative to WT. (C) Semi-quantitative RT-PCR with primers specific for genes identified in the microarray. RT-PCR was performed on RNA isolated from dorsal skin of WT (+/+), triple HET (+/−) and triple KO (−/−) mice. (D) In situ zymography assay demonstrates decreased proteolytic activity, indicated by reduction in green fluorescence, in triple KO epidermis. As a control, addition of the serine protease inhibitor aprotinin reduces fluorescent signal in both WT and triple KO (bottom panels). Note nuclear retention in cornified layers of the triple KO (white arrows). Bar: 50 μm.

layers of the stratum corneum of the triple KO mice (Fig. 6 A). Further analysis by immunoelectron microscopy confirmed retention of corneodesmosin in the upper layers of the triple KO epidermis: labeling was almost undetectable above corneocyte layer 11 of WT epidermis, but was still evident in corneocyte layer 17 of triple KO stratum corneum (Fig. 6 C).

We hypothesized that the decreased epidermal protease activity could also affect processing of profilaggrin. Profilaggrin is synthesized as a large insoluble phosphoprotein that accumulates in keratohyalin granules. Proteolysis liberates filaggrin monomers that aggregate keratin filaments, causing granular layer keratinocytes to collapse into flattened squames (Gan et al., 1990).

Immunoblotting of insoluble protein extracts from triple KO skin showed that the levels of unprocessed and incompletely processed profilaggrin were 1.4-fold higher in triple KO than in WT and triple HET skin; however, the levels of monomer were not significantly decreased (Fig. 6 B). Immunofluorescence microscopy revealed retention of the epitopes recognized by the filaggrin antiserum in triple KO stratum corneum (Fig. 6 A), but not in that of the single knockouts (Fig. S3 B).

Using immunoelectron microscopy, profilaggrin was detected in keratohyalin granules of both WT and triple KO epidermis and had a diffuse staining pattern in the lower stratum corneum (Fig. 6 D). In the middle layers (corneocytes 5–8) of the WT stratum corneum, detection of filaggrin was gradually lost, consistent with its processing into free amino acids (Scott et al., 1982) (Fig. 6 D). However, in triple KO stratum corneum relatively high levels of filaggrin were detected in these layers, providing further evidence for defective processing (Fig. 6 D). It is thus possible that defective processing of filaggrin into free amino acids accounts for the similar levels of filaggrin monomer observed in triple KO and WT epidermis (Fig. 6 B).

Inflammation in triple KO skin

It has recently been shown that null alleles of the *filaggrin* gene are associated with atopic dermatitis, establishing a role for impaired barrier function in the development of a chronic inflammatory skin disease (Palmer et al., 2006). The cytokine milieu in skin of atopic dermatitis patients prevents the induction of innate immune response genes due to higher levels of Th2 cytokines and lower levels of Th1 cytokines, such as interferon γ (Nomura et al., 2003). Microarray analysis indicated that 24% of the down-regulated genes in the triple KO skin were related to immune responses. Of these genes, 30% were related to innate immunity and 30% were interferon inducible, suggestive of a decrease in expression of, or responsiveness to, Th1 cytokines. We therefore examined the T lymphocyte populations present in the epidermis of triple KO mice by whole-mount labeling of tail epidermis.

Published December 31, 2007

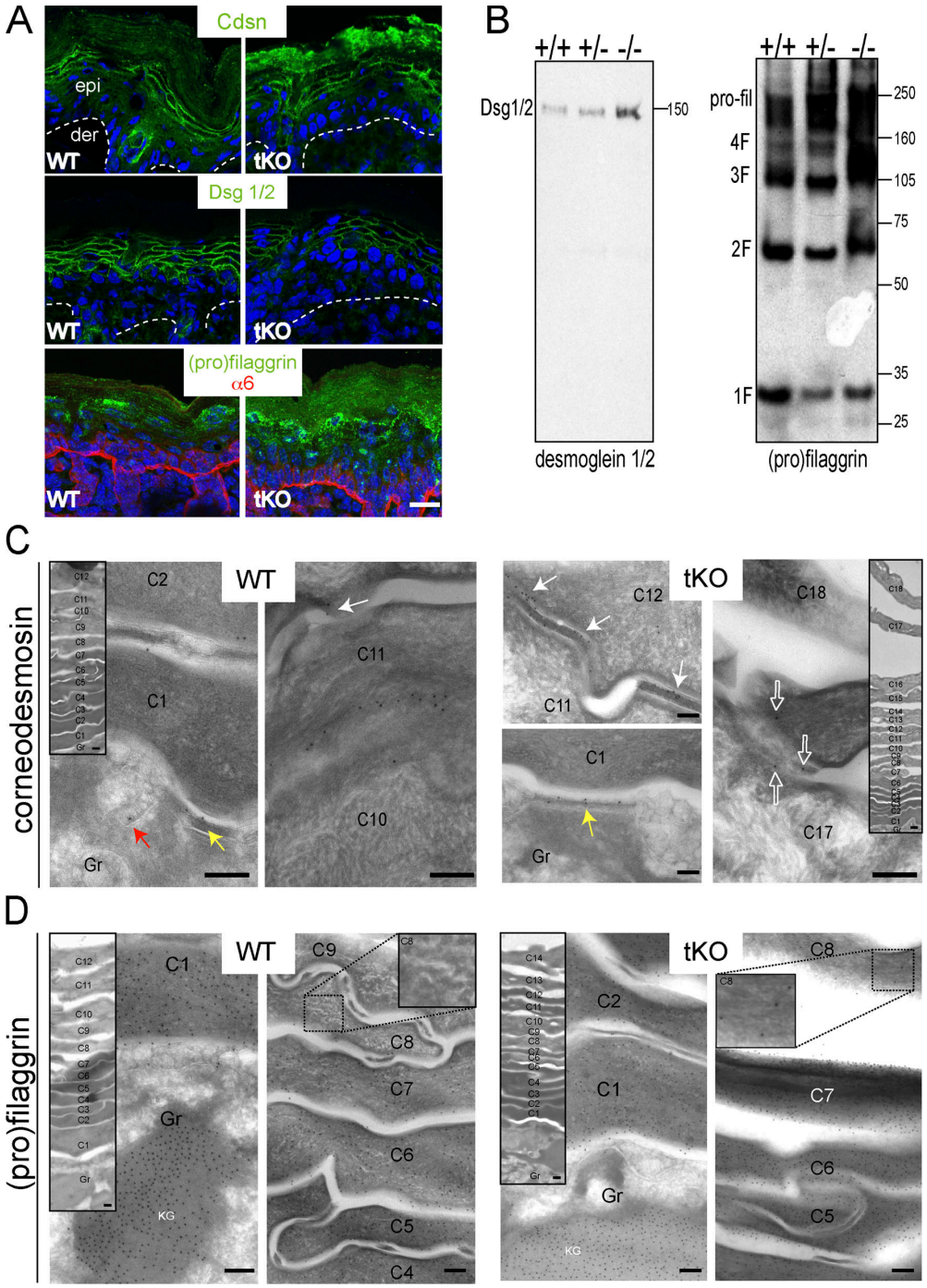

Figure 6. **Retention of desmoglein 1/2 and corneodesmosin and defective filaggrin processing in triple KO epidermis.** (A) Immunofluorescence staining of sections of WT or triple KO (tKO) P5 newborn skin with antibodies specific for corneodesmosin (Cdsn), desmoglein 1/2 (Dsg1/2), or (pro)filaggrin. The basal layer of the epidermis is marked with broken lines or immunostaining for α6 integrin (red). Nuclei are visualized with DAPI (blue). Bar: 20 μm. (B) Equal amounts of insoluble protein extracts from WT (+/+), triple HET (+/−), and triple KO (−/−) skin were separated by SDS-PAGE under reducing conditions and subjected to immunoblotting with antibodies specific for desmoglein 1/2 (left) or (pro)filaggrin (right). Increased levels of desmoglein 1/2 in insoluble protein extracts from triple KO suggest a delay in degradation. Filaggrin monomer (1F), dimer (2F), trimer (3F), tetramer (4F), and pro-filaggrin (pro-fil) are indicated (right). Note the increased levels of the high molecular weight processing intermediates (>2F) in the triple KO relative to triple HET or WT. Positions of molecular weight markers (kD) are indicated. (C) Immunoelectron microscopy of P5 newborn skin with antibodies specific for corneodesmosin. C1 to C18 designate the cornified cell layers, with C1 being adjacent to the granular layer and C18 being nearest the skin surface. Corneodesmosin is present in lamellar granules (red arrow) in granular keratinocytes and in desmosomes (yellow arrow) in the interface between the granular layer and the stratum corneum. Corneodesmosin is almost undetectable above the eleventh corneocyte layer in WT, but is abundant at this level in triple KO (white arrows; C11), and is still detectable up to the seventeenth corneocyte layer in triple KO (open arrows; C17). Bars: 200 nm. (D) Immuno-electron microscopy of P5 newborn skin with antibodies specific for (pro)filaggrin. (Pro)filaggrin detection in keratohyalin granules in the granular layer is similar in triple KO and WT. In WT stratum corneum, filaggrin staining is lost progressively from the innermost layer (C1) and is completely absent in C8. Filaggrin staining is retained in triple KO stratum corneum and is still detectable in C8. Insets are of CE layers (left) or magnified views of boxed areas (right). Gr: granular keratinocyte, KG: keratohyalin granule. Bars: 200 nm.

Published December 31, 2007

By double labeling epidermal whole mounts with antibodies to keratin 14 we could evaluate hair follicle morphology while simultaneously examining T cell populations (Fig. 7, A and B). Although involucrin, envoplakin, and periplakin are expressed in the inner root sheath of the hair follicle, the majority of hair follicles had a normal morphology and growth cycle (unpublished data), the only exception being that triple KO hair follicles had an enlarged infundibulum (Fig. 7, A–D).

Staining with antibodies specific for CD3 revealed a dramatic redistribution of T cells in triple KO skin relative to the WT and single knockout controls (Fig. 7 A and Fig. S3 C). Dendritic epidermal T cells (DETCs) are a subset of T cells normally resident in the skin that express the γδ T cell receptor and extend membrane processes to physically interact with keratinocytes, monitoring for damage and disease (Komori et al., 2006). In WT tail epidermis, $CD3^+$ $\gamma\delta^+$ DETCs could be observed at the edges of the parakeratotic scales that encompass hair follicle triplets (Fig. 7, A, C, and D). However, in triple KO epidermis, the $CD3^+$ $\gamma\delta^+$ DETCs were greatly reduced in number, with the few remaining cells localizing to the infundibulum of hair follicles (Fig. 7 D).

No increase in $CD8^+$ T cells was observed in the triple KO skin (unpublished data). However, there was a massive infiltrate of $CD3^+CD4^+$ T cells around the hair follicle infundibulum as well as in the dermis (Fig. 7, B–E). This infiltrate was not observed in the skin of WT or single KO mice (Fig. 7 E and Fig. S3 C).

Discussion

We have generated mice lacking the three proteins that form the scaffold onto which the epidermal CE is assembled. The triple KOs showed delayed barrier acquisition during embryonic development, defects in the assembled CE, and excessive accumulation of cornified layers (hyperkeratosis) throughout postnatal life. In addition, there was an accumulation of $CD3^+CD4^+$ T cells in the skin and a decrease in $\gamma\delta^+$ T cells (DETC). $\gamma\delta^+$ T cells are thought to play a role in controlling inflammatory responses driven by conventional $\alpha\beta^+$ T cells and are profoundly reduced in patients with atopic dermatitis (Katsuta et al., 2006).

Some features of the triple KO epidermis were consistent with the known functions of the proteins. Periplakin and envoplakin are constituents of the desmosomal plaques in the viable suprabasal epidermal layers and in triple KO epidermis the plaques exhibited decreased electron density. It is also possible that the abnormal morphology of corneodesmosomes was a direct consequence of the absence of these proteins. Loss of involucrin, envoplakin, and periplakin was predicted to disturb CE formation. In triple KO epidermis the first cornified cell layer had a reduction in the peripheral electron-dense line that is the hallmark of a fully formed CE and, in addition, the mechanical integrity of CEs was reduced.

Consistent with envoplakin, periplakin, and involucrin being key epidermal substrates for covalent attachment of ω-hydroxyceramides (Marekov and Steinert, 1998), there was reduced incorporation of lipids in the cornified layers. Although we did not exclude the possibility that the composition of lipids in the triple KO epidermis is altered, there was no evidence from our microarray analysis that expression of enzymes involved in CE lipid metabolism was affected.

The fact that the phenotype of the triple KO mice was not observed in any of the single knockouts or in triple HET animals supports earlier predictions of compensatory redundancy of the CE scaffold proteins. In the case of loricrin-null mice, the CE structural proteins Sprr2D, Sprr2H, and repetin were found to be up-regulated shortly after birth (Koch et al., 2000). Surprisingly, the only CE gene with altered gene expression identified in our analysis was *Lce1d* (2.331-fold greater in triple KO), and no changes were observed in the expression of genes for desmosome components.

Instead, compensation for the defects in the barrier was achieved by reduced desquamation. This mechanism has been observed in other models characterized by faulty barrier formation (Segre, 2006). Perhaps the clearest evidence comes from studies of *transglutaminase 1*. In humans, null mutations in the *transglutaminase 1* gene are associated with lamellar ichthyosis (Huber et al., 1995; Russell et al., 1995). *Transglutaminase 1*–deficient mice die at birth from dehydration (Matsuki et al., 1998), but if their skin is grafted onto nude mice it forms a hyperkeratotic stratum corneum and transepidermal water loss is restored to almost normal levels (Kuramoto et al., 2002). Mutation, gain or loss of expression of genes with a diverse range of known functions, including *Klf5*, *Arnt*, and *Fatp4*, results in both a defect in the epidermal barrier and hyperkeratosis (Herrmann et al., 2003; Geng et al., 2006; Sur et al., 2006).

A striking feature of the triple KO phenotype was up-regulation of the serine protease inhibitor *serpin a1b* and down-regulation of the proteases *cathepsin C*, *cathepsin S*, and *proteinase 3*, resulting in an overall decrease in epidermal proteolytic activity. Terminal differentiation is regulated by a cascade of proteases and protease inhibitors expressed in transitional layer cells during stratum corneum formation (Zeeuwen, 2004). Enzymes, such as transglutaminase 1, and structural proteins, such as filaggrin, require proteolytic processing to achieve full biological activity, and desquamation is facilitated by the degradation of corneodesmosome proteins (Guerrin et al., 1998; Simon et al., 2001). Thus, it is likely that the decreased protease activity in the triple KO epidermis is responsible for the delayed corneocyte shedding.

Although decreased epidermal proteolytic activity may compensate for a suboptimal barrier by reducing desquamation, dramatic changes in the balance between proteases and their inhibitors underlie several skin diseases (Zeeuwen, 2004). Null alleles of *cathepsin C* cause the autosomal recessive Papillon-Lefevre syndrome, a palmoplantar keratoderma, characterized by epidermal thickening and scaling (Toomes et al., 1999). Abnormally low epidermal proteolytic activity in mice deficient for the epithelial serine proteases Matriptase or Cap1/Prss8 results in neonatal lethality and severe barrier defects, including alterations in CE morphogenesis, desquamation and lipid matrix formation, and disrupted profilaggrin processing (List et al., 2003; Leyvraz et al., 2005). Conversely, hyperactivity of epidermal proteases, as in the human recessive inherited disease Netherton Syndrome, where patients have mutations in the *SPINK5* gene that encodes the LEKTI protease inhibitor, leads to severe skin

Published December 31, 2007

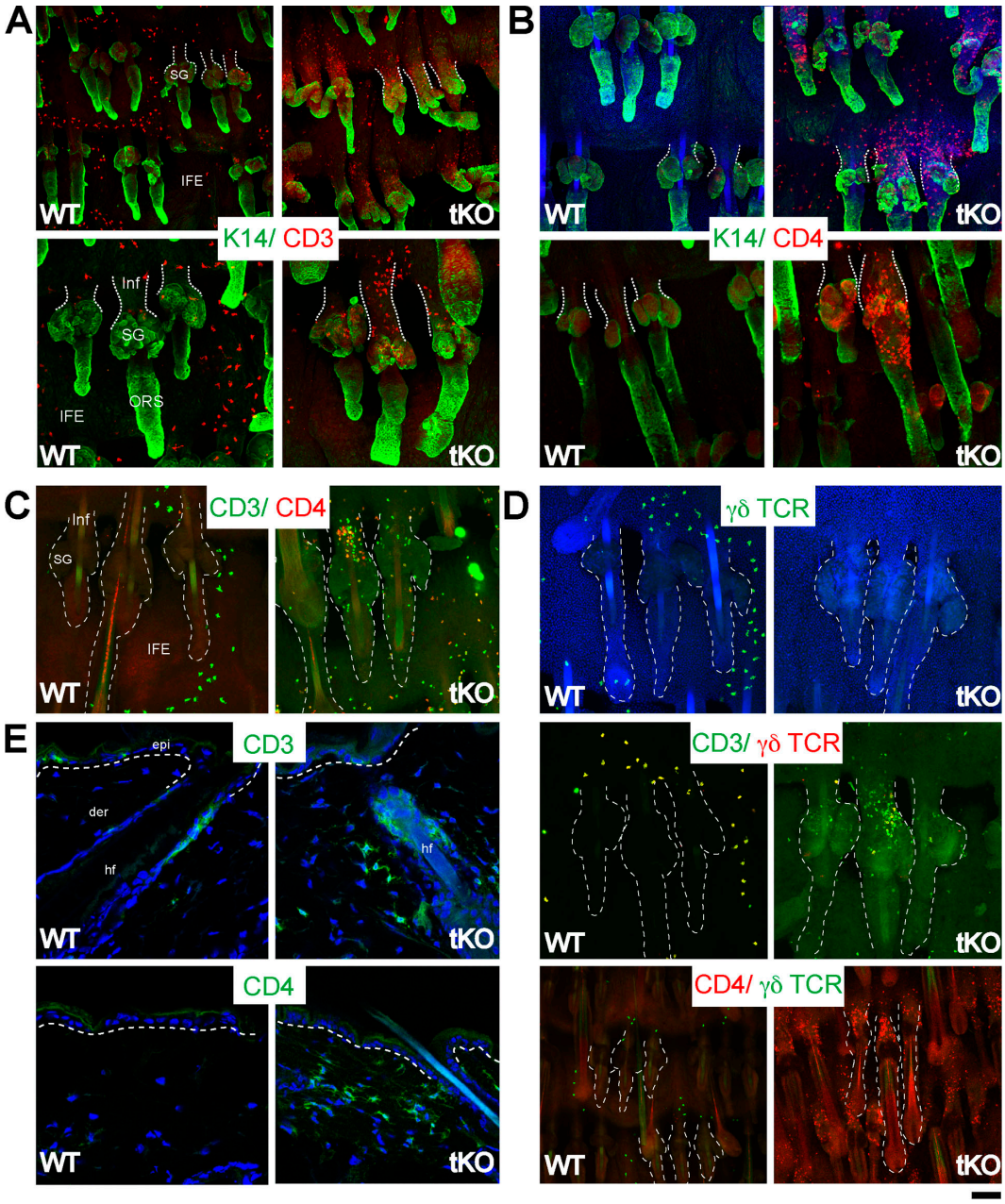

Figure 7. **Triple KO epidermis has a CD4$^+$ T cell infiltrate and a reduction in γδ$^+$ T cells.** (A) Immunostaining of tail epidermal whole mounts with antibodies specific for keratin 14 (green) and CD3 (red). Broken lines mark the hair follicle infundibulum (Inf). SG, sebaceous gland; IFE, interfollicular epidermis; ORS, outer root sheath. Bars: 50 μm (bottom panels) or 100 μm (top panels). (B) Immunostaining of tail epidermal whole mounts with antibodies specific for keratin 14 (green) and CD4 (red). Nuclei were counterstained with DAPI (blue). Broken lines mark the hair follicle infundibulum (Inf). Bars: 50 μm (bottom panels) or 100 μm (top panels). (C) Immunostaining of tail epidermal whole mounts with antibodies specific for CD3 (green) and CD4 (red). Yellow fluorescence indicates colocalization of CD3 and CD4 staining in the triple KO. Broken lines indicate hair follicles and sebaceous glands. Bar: 50 μm. (D) Immunostaining of tail epidermal whole mounts with antibodies specific for γδ TCR and CD3 (middle panels) or CD4 (bottom panels). In WT, CD3 and γδ TCR are perfectly colocalized (yellow), whereas γδ TCR staining is almost undetectable in triple KO. Bars: 50 μm (bottom panels) or 100 μm (top panels). (E) Immunostaining of sections of dorsal adult skin for CD3 or CD4 (green). Nuclei were visualized with DAPI (blue). Note the dermal infiltrate of CD3$^+$ and CD4$^+$ cells in the triple KO. Broken lines mark the basal layer of the epidermis. Hf, hair follicle; epi, epidermis; der, dermis. Bar: 20 μm.

barrier defects (Chavanas et al., 2000). In mice, loss of expression of Lekti results in neonatal lethality from dehydration, caused by loss of the skin barrier through premature corneodesmosome degradation (Yang et al., 2004; Descargues et al., 2005).

At present it is unclear whether cathepsin C, or the other proteases identified in the microarray, are involved directly in corneodesmosome degradation or indirectly in protease activation cascades. *Serpin alb* belongs to the α_1-antiproteinase/α_1-antitrypsin gene family and forms stable inhibitory complexes with trypsin, chymotrypsin, and elastase (Barbour et al., 2002). Potential targets of serpin alb in the epidermis include the serine proteases stratum corneum chymotryptic and trypic enzymes that mediate corneodesmosome degradation (Hansson et al., 1994; Caubet et al., 2004).

Published December 31, 2007

One of the most exciting recent discoveries in the epidermal barrier field has been the linkage of loss-of-function mutations in the *filaggrin* gene, found in ~9% of the European population, to ichthyosis vulgaris, a skin disorder characterized by dry scaly skin and mild hyperkeratosis, as well as to atopic dermatitis (Palmer et al., 2006; Smith et al., 2006). Triple KO epidermis differed from that of ichthyosis vulgaris patients and filaggrin processing mutant mice (Presland et al., 2000) because the granular layer was unaffected and cell flattening still occurred in the first cornified layers. This suggests that the decreased profilaggrin processing in the triple KO is not solely responsible for their phenotype; it could, nevertheless, contribute to the dry, scaly skin because natural moisturizing factor, a complex mixture of low molecular weight, water-soluble compounds formed in corneocytes, is generated by proteolysis of deiminated filaggrin (Rawlings and Harding, 2004).

It is thought that atopic dermatitis patients have a faulty barrier that is more permissive to entry of allergens, antigens, and chemicals from the environment, thus provoking inflammation (Irvine and McLean, 2006). Our data support the link between a defective barrier and alterations in the immune compartment of the skin. It is also possible that the decreased epidermal protease activity in triple KO mice generates fewer antimicrobial peptides, rendering the mice more susceptible to infection (Yamasaki et al., 2006). Antimicrobial peptides are produced at lower levels in the skin of atopic dermatitis patients, and it would be interesting to examine whether epidermal proteolysis is decreased in these individuals (Nomura et al., 2003; Howell et al., 2006).

The mechanism by which loss of envoplakin, periplakin, and involucrin triggers an immunological phenotype requires further investigation. Approximately 7% of down-regulated genes identified in the microarray analysis are interferon inducible. It is possible that the decrease in their expression is linked to lower interferon γ levels in the triple KO epidermis, which could not only trigger proliferation of Th2 lymphocytes, but could lead to reduced cathepsin S expression (Schwarz et al., 2002).

Atopic disease, including atopic dermatitis, allergy, and asthma, affects ~10–20% of the population in the developed world (Leung et al., 2004). It has been predicted that in addition to variants in *filaggrin*, variants in other epidermal differentiation complex (1q21) genes might be involved in the pathogenesis of atopic dermatitis and asthma (Palmer et al., 2006). Mutations in the CE scaffold proteins alone or in combination with the common *filaggrin* mutations may play a role in these diseases, but only the gene for *involucrin* lies within 1q21. Interestingly, the *envoplakin* gene is located on chromosome 17q25, a region previously identified as having linkage to atopic dermatitis (Cookson et al., 2001). Overall, our data lead us to speculate that polymorphisms in *involucrin*, *envoplakin*, and *periplakin* may contribute to susceptibility to pathological human skin conditions such as ichthyosis vulgaris and atopic dermatitis.

Materials and methods

Generation of mice and animal protocols

Triple KO mice were generated by crossing the single knockout mice for *envoplakin* (Määttä et al., 2001), *involucrin* (Djian et al., 2000), and *periplakin* (Aho et al., 2004). All of the single knockouts were created in the 129 background (*envoplakin*, 129(P2)Ola; *involucrin*, 129S4/SvJae; *periplakin*, 129S1/SvImJ) and were crossed onto C57BL/6. WT controls were age- and sex-matched C57BL/6. Triple HET controls were generated by breeding triple KOs with C57BL/6 mice. All protocols used in this study were approved by the local animal ethics and genetic modification committees at Cancer Research UK and covered by a Home Office project license.

Southern blotting

Southern blotting was performed on genomic DNA isolated from tail snips and digested overnight with BamHI (*envoplakin*), PstI (*involucrin*), or SacI (*periplakin*). Blots were probed with gene-specific radiolabeled probes for *envoplakin* (Määttä et al., 2001), *involucrin* (Djian et al., 2000), and *periplakin* (Aho et al., 2004).

Antibodies

The following mouse monoclonal antibodies were used at the dilutions stated: F27.28 (anti-corneodesmosin; 2.5 μg/ml; a gift of Prof. G. Serre, CNRS-UPS UMR5165, Toulouse, France; [Serre et al., 1991]), DG3.10 (anti-desmoglein 1/2; 2.5 μg/ml;), 115F (1:50; anti-desmoplakin; gift of D.R. Garrod, University of Manchester, Manchester, UK), anti-occludin (1:100; Invitrogen). The following rat monoclonal antibodies were used at the dilutions stated: GoH3 (anti-α6 integrin; 1:500; BD Biosciences), 17A2 AlexaFluor 488 (anti-CD3; 1:200; BD Biosciences), GK1.5 AlexaFluor 647 (anti-CD4; 1:200; BioLegend), ECCD-1 (1:100; anti-E-cadherin; Invitrogen). The Armenian hamster monoclonal antibody GL3 (BD Biosciences) specific for γδ TCR was used at 1:200. The following rabbit antisera were used at the dilutions stated: anti-desmoplakin (1:100; Research Diagnostics, Inc.), ERLI3 (anti-involucrin; 1:10,000; [Li et al., 2000], and TD2 (anti-periplakin; 1:500; [DiColandrea et al., 2000]). Rabbit antisera specific for mouse (pro)filaggrin, loricrin, and keratins 1, 10, and 14 were from Covance Research Products, Inc. and were used at 1:1,000. A peptide corresponding to C-terminal amino acids 2014–2033 (AMLEGYRCYRAASPTLPRSC) of mouse envoplakin was used to generate rabbit antiserum LS5 (1:1,000).

For immunofluorescence, AlexaFluor 488–, 594–, or 633–conjugated goat anti–rabbit or anti–mouse IgG (Invitrogen) were diluted at 1:1,000 and used for detection of primary antibodies. FITC-conjugated goat anti–Armenian hamster (The Jackson Laboratory) was diluted 1:1,000. For immunoblotting, HRP-conjugated donkey anti–rabbit or anti–mouse IgG was used at 1:4,000 (GE Healthcare).

Histology, immunofluorescence staining, and microscopy

Unless otherwise mentioned, all chemicals were from Sigma-Aldrich. Tissues were fixed in formal saline and embedded in paraffin. For frozen sections, tissues were placed in OCT compound in a liquid nitrogen–cooled isopentane bath. For routine histology, 5-μm sections were stained with hematoxylin and eosin. Images of hematoxylin and eosin–stained sections were obtained at room temperature using a microscope (Eclipse 90i; Nikon) equipped with the Nikon DS-Fil camera and Nikon CFI Plan Fluor 10× (NA 0.30, air correction), CFI Plan Apochromat 20× (NA 0.75, air correction), and CFI Plan Fluor 40× (NA 1.30, oil correction) objectives. NIS-Elements software was used for image acquisition.

For immunofluorescence staining, frozen tissue sections (5 μm) were fixed with 4% paraformaldehyde/PBS for 10 min followed by permeabilization with 0.2% Triton X-100/PBS for 5 min at room temperature, blocking with 5% donkey serum and 0.5% fish skin gelatin in PBS and immunolabeling. Whole mounts of tail epidermal sheets were prepared and immunolabeled as described (Braun et al., 2003). Nile Red was used at 1 ng/ml to detect lipids. DAPI (Invitrogen) was used to stain nuclei.

Images of fluorescently labeled specimens were taken at room temperature using the LSM 510 laser scanning confocal microscope equipped with 405-, 488-, 594-, and 633-nm lasers (Carl Zeiss, Inc.). LSM 510 software was used to acquire images using the following immersion lenses (Carl Zeiss, Inc.): 10× C-Aprochromat (NA 0.45; water correction), 25× Plan-Neofluar (NA 0.80; immersion correction), 40× C-Aprochromat (NA 1.2; water correction). Three-dimensional reconstructions of z-stacks were performed using LSM 510 software. All images were further processed using Adobe Photoshop CS2 and compiled using Adobe Illustrator CS2.

Electron microscopy

For transmission electron microscopy, adult mouse dorsal skin was fixed in 2.5% glutaraldehyde and 4% paraformaldehyde in Sorensen's buffer (pH 7.4). The tissues were embedded in araldite resin and 100-nm sections were cut on a Reichert Ultracut S ultramicrotome. Sections were stained with 1.5% uranyl acetate and lead citrate.

Immunogold electron microscopy was performed on thin sections of high pressure-frozen and freeze-substituted P5 dorsal skin. Skin was fixed

Published December 31, 2007

with 2% paraformaldehyde/PBS, then treated with 100 mM glycine/PBS. Samples were incubated in 2.3 M sucrose/0.1 M phosphate buffer, pH 7.4, for 2 d at 4°C, mounted on aluminium pins, and cryofixed by immersing into liquid propane cooled to −190°C (Reichert KF80 cryo-fixation apparatus). Sections (~90 nm) were cut at −120°C using the Leica EM FC6 cryo-ultramicrotome and retrieved with 2.3 M sucrose/0.1 M phosphate buffer, pH 7.4, onto nickel grids covered with Formvar support film. Immunostaining was performed at room temperature. Specimen-mounted grids were incubated for 15 min with 1% BSA/PBS, and then 1 h with antibodies specific for (pro)filaggrin or corneodesmosin. After washing with 1% BSA/PBS, sections were incubated for 30 min with secondary antibodies conjugated to 10-nm colloidal gold particles. Sections were post-fixed in 1% glutaraldehyde/PBS for 5 min, followed by staining with 2% neutral uranyl acetate for 10 min and embedding in a solution of 1.5% polyvinyl alcohol and 1.5% uranyl acetate.

Specimens were analyzed at room temperature and images were taken using an electron microscope (model 1010; JEOL) equipped with a US1000 camera (Gatan) using Digital Micrograph software (Gatan). All images were further processed using Adobe Photoshop CS2 and compiled using Adobe Illustrator CS2.

Dye exclusion assay for development of epidermal barrier

Mouse embryos were dehydrated by 1-min incubations in an ascending series of methanol, rehydrated with the same methanol series, washed in PBS, and stained with 0.0125% toluidine blue as described (Hardman et al., 1998). Higher magnification images of embryos were taken with a stereomicroscope (model MZAPO; Leica), with a camera (model DC500; Leica) and Firecam software (Leica). Lower magnification images of embryos were taken using a digital camera (model EO5 D30; Canon).

Isolation and analysis of cornified envelopes

CEs were isolated from mouse ear tips as previously described (Määttä et al., 2001). For sonication experiments, the CE suspension was sonicated in a Branson 250 cup sonicator at 4°C for various time points (Koch et al., 2000). After sonication, intact CEs were counted using a haemocytometer. Experiments were performed on CEs isolated from at least three mice per genotype. Images of CEs were taken at room temperature with an inverted microscope (Diaphot 300; Nikon) fitted with an Orca CCD camera (Hamamatsu) and a 10× Nikon DL objective (NA 0.25, air correction). AQM6 software was used to acquire images (Kinetic Imaging).

Microarrays

Preparation of samples for microarray analysis was performed as described (Silva-Vargas et al., 2005), using RNA isolated from dorsal skin of 7-wk-old female mice (quadruplicate samples from WT, triple HET, or triple KO) and the Genechip Mouse Genome 430 2.0 Array (Affymetrix). Microarray data were analyzed with GeneSpring software (Agilent Technologies). Signal intensities were extracted from the CEL files and normalized by RMA algorithms. Raw data were filtered with signal intensities >150, genes twofold changed in triple KO versus WT with a 0.05 P-value in at least one replicate.

Semi-quantitative RT-PCR

Total RNA was prepared from mouse skin using TriReagent. cDNA was generated using the SuperScript First-Strand Synthesis System (Invitrogen). Primer sequences are listed in Table S2 (available at http://www.jcb.org/cgi/content/full/jcb.200706187/DC1).

In situ zymography

Frozen sections (8 μm) were rinsed with 1% Tween 20 and incubated at 37°C for 2 h with 1 μg/ml BODIPY-Fl-casein (Invitrogen). Aprotinin (1 μM) was added to some sections as a control. Sections were rinsed with 1% Tween 20, mounted, and examined immediately with the Leica TCS Sp5 confocal microscope with a 40× HCX PL APO objective (NA 1.25, oil correction) or a 63× HCX PL APO objective (NA 1.4, oil correction). Leica LAS AF software was used for image acquisition and for subsequent quantification of fluorescence intensity.

Western blotting

Protein extracts were isolated from adult mouse dorsal skin. For the detection of (pro)filaggrin, skin was homogenized in protein extraction buffer (40 mM Tris-HCl, pH 7.5, 10 mM EDTA) containing protease inhibitors and 0.5% Nonidet P-40. Detergent-soluble and -insoluble protein fractions were separated by centrifugation. The detergent-insoluble pellet was solubilized in protein extraction buffer containing 8M urea and 50 mM dithiothreitol as described (Simon et al., 1997). Protein concentrations were measured using the Coomassie Plus protein assay (Pierce Chemical Co.) and equal amounts of protein were resolved by 10% SDS-PAGE before transfer to Hybond nitrocellulose membrane (GE Healthcare). Membranes were probed with primary and HRP-conjugated secondary antibodies and visualized with ECL (GE Healthcare). Band intensities were quantified using ImageJ software (National Institutes of Health, Bethesda, MD).

Online supplemental material

Figure S1 shows confirmation of gene targeting in triple KO mice by Southern blotting and immunofluorescence microscopy. Figure S2 shows that single KO mice do not have hyperkeratosis or reduced epidermal lipid content. Figure S3 shows that substantial reductions in stratum corneum proteolytic activity and (pro)filaggrin degradation, and an increase in $CD3^+$ and $CD4^+$ dermal lymphocytes are features of the triple knockouts but not the single knockouts. Table S1 contains the genes identified as having altered expression (greater than twofold up-regulated or down-regulated) in triple KO mice. Table S2 lists the oligonucleotide primers used for semi-quantitative RT-PCR. Online supplemental material is available at http://www.jcb.org/cgi/content/full/jcb.200706187/DC1.

We thank the Histopathology, Electron Microscopy, Light Microscopy, and Biological Resources facilities of Cancer Research UK for superb technical assistance. We are most grateful to Howard Green for his encouragement and comments.

This work was funded by Cancer Research UK; the National Institutes of Health, US Public Health Service; EuroStemCell; and a grant to A. Määttä from the BBSRC. L.M. Sevilla was the recipient of a National Institutes of Health fellowship (HD42379-02).

Submitted: 26 June 2007
Accepted: 26 November 2007

References

Aho, S., K. Li, Y. Ryoo, C. McGee, A. Ishida-Yamamoto, J. Uitto, and J.F. Klement. 2004. Periplakin gene targeting reveals a constituent of the cornified cell envelope dispensable for normal mouse development. *Mol. Cell. Biol.* 24:6410–6418.

Amagai, M., K. Ishii, T. Hashimoto, S. Gamou, N. Shimizu, and T. Nishikawa. 1995. Conformational epitopes of pemphigus antigens (Dsg1 and Dsg3) are calcium dependent and glycosylation independent. *J. Invest. Dermatol.* 105:243–247.

Barbour, K.W., R.L. Goodwin, F. Guillonneau, Y. Wang, H. Baumann, and F.G. Berger. 2002. Functional diversification during evolution of the murine alpha(1)-proteinase inhibitor family: role of the hypervariable reactive center loop. *Mol. Biol. Evol.* 19:718–727.

Basel-Vanagaite, L., R. Attia, A. Ishida-Yamamoto, L. Rainshtein, D. Ben Amitai, R. Lurie, M. Pasmanik-Chor, M. Indelman, A. Zvulunov, S. Saban, et al. 2007. Autosomal recessive ichthyosis with hypotrichosis caused by a mutation in ST14, encoding type II transmembrane serine protease matriptase. *Am. J. Hum. Genet.* 80:467–477.

Braun, K.M., C. Niemann, U.B. Jensen, J.P. Sundberg, V. Silva-Vargas, and F.M. Watt. 2003. Manipulation of stem cell proliferation and lineage commitment: visualisation of label-retaining cells in wholemounts of mouse epidermis. *Development.* 130:5241–5255.

Brown, S.J., C.M. Tilli, B. Jackson, A.A. Avilion, M.C. Macleod, L.J. Maltais, R.C. Lovering, and C. Byrne. 2007. Rodent Lce gene clusters: new nomenclature, gene organization, and divergence of human and rodent genes. *J. Invest. Dermatol.* 127:1782–1786.

Candi, E., R. Schmidt, and G. Melino. 2005. The cornified envelope: a model of cell death in the skin. *Nat. Rev. Mol. Cell Biol.* 6:328–340.

Caubet, C., N. Jonca, M. Brattsand, M. Guerrin, D. Bernard, R. Schmidt, T. Egelrud, M. Simon, and G. Serre. 2004. Degradation of corneodesmosome proteins by two serine proteases of the kallikrein family, SCTE/KLK5/hK5 and SCCE/KLK7/hK7. *J. Invest. Dermatol.* 122:1235–1244.

Chavanas, S., C. Bodemer, A. Rochat, D. Hamel-Teillac, M. Ali, A.D. Irvine, J.L. Bonafe, J. Wilkinson, A. Taieb, Y. Barrandon, et al. 2000. Mutations in SPINK5, encoding a serine protease inhibitor, cause Netherton syndrome. *Nat. Genet.* 25:141–142.

Cookson, W.O., B. Ubhi, R. Lawrence, G.R. Abecasis, A.J. Walley, H.E. Cox, R. Coleman, N.I. Leaves, R.C. Trembath, M.F. Moffatt, and J.I. Harper. 2001. Genetic linkage of childhood atopic dermatitis to psoriasis susceptibility loci. *Nat. Genet.* 27:372–373.

Descargues, P., C. Deraison, C. Bonnart, M. Kreft, M. Kishibe, A. Ishida-Yamamoto, P. Elias, Y. Barrandon, G. Zambruno, A. Sonnenberg, and

A. Hovnanian. 2005. Spink5-deficient mice mimic Netherton syndrome through degradation of desmoglein 1 by epidermal protease hyperactivity. *Nat. Genet.* 37:56–65.

DiColandrea, T., T. Karashima, A. Maatta, and F.M. Watt. 2000. Subcellular distribution of envoplakin and periplakin: insights into their role as precursors of the epidermal cornified envelope. *J. Cell Biol.* 151:573–586.

Djian, P., K. Easley, and H. Green. 2000. Targeted ablation of the murine involucrin gene. *J. Cell Biol.* 151:381–388.

Elias, P.M., D. Crumrine, U. Rassner, J.P. Hachem, G.K. Menon, W. Man, M.H. Choy, L. Leypoldt, K.R. Feingold, and M.L. Williams. 2004. Basis for abnormal desquamation and permeability barrier dysfunction in RXLI. *J. Invest. Dermatol.* 122:314–319.

Gan, S.Q., O.W. McBride, W.W. Idler, N. Markova, and P.M. Steinert. 1990. Organization, structure, and polymorphisms of the human profilaggrin gene. *Biochemistry.* 29:9432–9440.

Geng, S., A. Mezentsev, S. Kalachikov, K. Raith, D.R. Roop, and A.A. Panteleyev. 2006. Targeted ablation of Arnt in mouse epidermis results in profound defects in desquamation and epidermal barrier function. *J. Cell Sci.* 119:4901–4912.

Ghadially, R., M.L. Williams, S.Y. Hou, and P.M. Elias. 1992. Membrane structural abnormalities in the stratum corneum of the autosomal recessive ichthyoses. *J. Invest. Dermatol.* 99:755–763.

Groot, K.R., L.M. Sevilla, K. Nishi, T. DiColandrea, and F.M. Watt. 2004. Kazrin, a novel periplakin-interacting protein associated with desmosomes and the keratinocyte plasma membrane. *J. Cell Biol.* 166:653–659.

Guerrin, M., M. Simon, M. Montezin, M. Haftek, C. Vincent, and G. Serre. 1998. Expression cloning of human corneodesmosin proves its identity with the product of the S gene and allows improved characterization of its processing during keratinocyte differentiation. *J. Biol. Chem.* 273:22640–22647.

Hansson, L., M. Stromqvist, A. Backman, P. Wallbrandt, A. Carlstein, and T. Egelrud. 1994. Cloning, expression, and characterization of stratum corneum chymotryptic enzyme. A skin-specific human serine proteinase. *J. Biol. Chem.* 269:19420–19426.

Hardman, M.J., P. Sisi, D.N. Banbury, and C. Byrne. 1998. Patterned acquisition of skin barrier function during development. *Development.* 125:1541–1552.

Herrmann, T., F. van der Hoeven, H.J. Grone, A.F. Stewart, L. Langbein, I. Kaiser, G. Liebisch, I. Gosch, F. Buchkremer, W. Drobnik, et al. 2003. Mice with targeted disruption of the fatty acid transport protein 4 (Fatp 4, Slc27a4) gene show features of lethal restrictive dermopathy. *J. Cell Biol.* 161:1105–1115.

Howell, M.D., R.L. Gallo, M. Boguniewicz, J.F. Jones, C. Wong, J.E. Streib, and D.Y. Leung. 2006. Cytokine milieu of atopic dermatitis skin subverts the innate immune response to vaccinia virus. *Immunity.* 24:341–348.

Huber, M., I. Rettler, K. Bernasconi, E. Frenk, S.P. Lavrijsen, M. Ponec, A. Bon, S. Lautenschlager, D.F. Schorderet, and D. Hohl. 1995. Mutations of keratinocyte transglutaminase in lamellar ichthyosis. *Science.* 267:525–528.

Irvine, A.D., and W.H. McLean. 2006. Breaking the (un)sound barrier: filaggrin is a major gene for atopic dermatitis. *J. Invest. Dermatol.* 126:1200–1202.

Jefferson, J.J., C.L. Leung, and R.K. Liem. 2004. Plakins: goliaths that link cell junctions and the cytoskeleton. *Nat. Rev. Mol. Cell Biol.* 5:542–553.

Kalinin, A.E., A.V. Kajava, and P.M. Steinert. 2002. Epithelial barrier function: assembly and structural features of the cornified cell envelope. *Bioessays.* 24:789–800.

Karashima, T., and F.M. Watt. 2002. Interaction of periplakin and envoplakin with intermediate filaments. *J. Cell Sci.* 115:5027–5037.

Katsuta, M., Y. Takigawa, M. Kimishima, M. Inaoka, R. Takahashi, and T. Shiohara. 2006. NK cells and gamma delta+ T cells are phenotypically and functionally defective due to preferential apoptosis in patients with atopic dermatitis. *J. Immunol.* 176:7736–7744.

Kazerounian, S., J. Uitto, and S. Aho. 2002. Unique role for the periplakin tail in intermediate filament association: specific binding to keratin 8 and vimentin. *Exp. Dermatol.* 11:428–438.

Koch, P.J., P.A. de Viragh, E. Scharer, D. Bundman, M.A. Longley, J. Bickenbach, Y. Kawachi, Y. Suga, Z. Zhou, M. Huber, et al. 2000. Lessons from loricrin-deficient mice: compensatory mechanisms maintaining skin barrier function in the absence of a major cornified envelope protein. *J. Cell Biol.* 151:389–400.

Komori, H.K., T.F. Meehan, and W.L. Havran. 2006. Epithelial and mucosal gamma delta T cells. *Curr. Opin. Immunol.* 18:534–538.

Kuramoto, N., T. Takizawa, T. Takizawa, M. Matsuki, H. Morioka, J.M. Robinson, and K. Yamanishi. 2002. Development of ichthyosiform skin compensates for defective permeability barrier function in mice lacking transglutaminase 1. *J. Clin. Invest.* 109:243–250.

Leung, D.Y., M. Boguniewicz, M.D. Howell, I. Nomura, and Q.A. Hamid. 2004. New insights into atopic dermatitis. *J. Clin. Invest.* 113:651–657.

Leyvraz, C., R.P. Charles, I. Rubera, M. Guitard, S. Rotman, B. Breiden, K. Sandhoff, and E. Hummler. 2005. The epidermal barrier function is dependent on the serine protease CAP1/Prss8. *J. Cell Biol.* 170:487–496.

Li, E.R., D.M. Owens, P. Djian, and F.M. Watt. 2000. Expression of involucrin in normal, hyperproliferative and neoplastic mouse keratinocytes. *Exp. Dermatol.* 9:431–438.

List, K., R. Szabo, P.W. Wertz, J. Segre, C.C. Haudenschild, S.Y. Kim, and T.H. Bugge. 2003. Loss of proteolytically processed filaggrin caused by epidermal deletion of Matriptase/MT-SP1. *J. Cell Biol.* 163:901–910.

Määttä, A., T. DiColandrea, K. Groot, and F.M. Watt. 2001. Gene targeting of envoplakin, a cytoskeletal linker protein and precursor of the epidermal cornified envelope. *Mol. Cell. Biol.* 21:7047–7053.

Marekov, L.N., and P.M. Steinert. 1998. Ceramides are bound to structural proteins of the human foreskin epidermal cornified cell envelope. *J. Biol. Chem.* 273:17763–17770.

Marshall, D., M.J. Hardman, K.M. Nield, and C. Byrne. 2001. Differentially expressed late constituents of the epidermal cornified envelope. *Proc. Natl. Acad. Sci. USA.* 98:13031–13036.

Matsuki, M., F. Yamashita, A. Ishida-Yamamoto, K. Yamada, C. Kinoshita, S. Fushiki, E. Ueda, Y. Morishima, K. Tabata, H. Yasuno, et al. 1998. Defective stratum corneum and early neonatal death in mice lacking the gene for transglutaminase 1 (keratinocyte transglutaminase). *Proc. Natl. Acad. Sci. USA.* 95:1044–1049.

Nemes, Z., L.N. Marekov, L. Fesus, and P.M. Steinert. 1999. A novel function for transglutaminase 1: attachment of long-chain omega-hydroxyceramides to involucrin by ester bond formation. *Proc. Natl. Acad. Sci. USA.* 96:8402–8407.

Nomura, I., E. Goleva, M.D. Howell, Q.A. Hamid, P.Y. Ong, C.F. Hall, M.A. Darst, B. Gao, M. Boguniewicz, J.B. Travers, and D.Y. Leung. 2003. Cytokine milieu of atopic dermatitis, as compared to psoriasis, skin prevents induction of innate immune response genes. *J. Immunol.* 171:3262–3269.

Palmer, C.N., A.D. Irvine, A. Terron-Kwiatkowski, Y. Zhao, H. Liao, S.P. Lee, D.R. Goudie, A. Sandilands, L.E. Campbell, F.J. Smith, et al. 2006. Common loss-of-function variants of the epidermal barrier protein filaggrin are a major predisposing factor for atopic dermatitis. *Nat. Genet.* 38:441–446.

Presland, R.B., D. Boggess, S.P. Lewis, C. Hull, P. Fleckman, and J.P. Sundberg. 2000. Loss of normal profilaggrin and filaggrin in flaky tail (ft/ft) mice: an animal model for the filaggrin-deficient skin disease ichthyosis vulgaris. *J. Invest. Dermatol.* 115:1072–1081.

Rawlings, A.V., and C.R. Harding. 2004. Moisturization and skin barrier function. *Dermatol. Ther.* 17(Suppl 1):43–48.

Rice, R.H., and H. Green. 1977. The cornified envelope of terminally differentiated human epidermal keratinocytes consists of cross-linked protein. *Cell.* 11:417–422.

Rice, R.H., and H. Green. 1979. Presence in human epidermal cells of a soluble protein precursor of the cross-linked envelope: activation of the cross-linking by calcium ions. *Cell.* 18:681–694.

Robinson, N.A., S. Lapic, J.F. Welter, and R.L. Eckert. 1997. S100A11, S100A10, annexin I, desmosomal proteins, small proline-rich proteins, plasminogen activator inhibitor-2, and involucrin are components of the cornified envelope of cultured human epidermal keratinocytes. *J. Biol. Chem.* 272:12035–12046.

Roop, D.R., C.K. Cheng, L. Titterington, C.A. Meyers, J.R. Stanley, P.M. Steinert, and S.H. Yuspa. 1984. Synthetic peptides corresponding to keratin subunits elicit highly specific antibodies. *J. Biol. Chem.* 259:8037–8040.

Ruhrberg, C., M.A. Hajibagheri, M. Simon, T.P. Dooley, and F.M. Watt. 1996. Envoplakin, a novel precursor of the cornified envelope that has homology to desmoplakin. *J. Cell Biol.* 134:715–729.

Ruhrberg, C., M.A. Hajibagheri, D.A. Parry, and F.M. Watt. 1997. Periplakin, a novel component of cornified envelopes and desmosomes that belongs to the plakin family and forms complexes with envoplakin. *J. Cell Biol.* 139:1835–1849.

Russell, L.J., J.J. DiGiovanna, G.R. Rogers, P.M. Steinert, N. Hashem, J.G. Compton, and S.J. Bale. 1995. Mutations in the gene for transglutaminase 1 in autosomal recessive lamellar ichthyosis. *Nat. Genet.* 9:279–283.

Schwarz, G., W.H. Boehncke, M. Braun, C.J. Schroter, T. Burster, T. Flad, D. Dressel, E. Weber, H. Schmid, and H. Kalbacher. 2002. Cathepsin S activity is detectable in human keratinocytes and is selectively upregulated upon stimulation with interferon-gamma. *J. Invest. Dermatol.* 119:44–49.

Scott, I.R., C.R. Harding, and J.G. Barrett. 1982. Histidine-rich protein of the keratohyalin granules. Source of the free amino acids, urocanic acid and pyrrolidone carboxylic acid in the stratum corneum. *Biochim. Biophys. Acta.* 719:110–117.

Segre, J.A. 2006. Epidermal barrier formation and recovery in skin disorders. *J. Clin. Invest.* 116:1150–1158.

Serre, G., V. Mils, M. Haftek, C. Vincent, F. Croute, A. Reano, J.P. Ouhayoun, S. Bettinger, and J.P. Soleilhavoup. 1991. Identification of late differentiation antigens of human cornified epithelia, expressed in re-organized desmosomes and bound to cross-linked envelope. *J. Invest. Dermatol.* 97:1061–1072.

Silva-Vargas, V., C. Lo Celso, A. Giangreco, T. Ofstad, D.M. Prowse, K.M. Braun, and F.M. Watt. 2005. Beta-catenin and Hedgehog signal strength can specify number and location of hair follicles in adult epidermis without recruitment of bulge stem cells. *Dev. Cell.* 9:121–131.

Simon, M., and H. Green. 1984. Participation of membrane-associated proteins in the formation of the cross-linked envelope of the keratinocyte. *Cell.* 36:827–834.

Simon, M., M. Montezin, M. Guerrin, J.J. Durieux, and G. Serre. 1997. Characterization and purification of human corneodesmosin, an epidermal basic glycoprotein associated with corneocyte-specific modified desmosomes. *J. Biol. Chem.* 272:31770–31776.

Simon, M., N. Jonca, M. Guerrin, M. Haftek, D. Bernard, C. Caubet, T. Egelrud, R. Schmidt, and G. Serre. 2001. Refined characterization of corneodesmosin proteolysis during terminal differentiation of human epidermis and its relationship to desquamation. *J. Biol. Chem.* 276:20292–20299.

Skerrow, C.J., D.G. Clelland, and D. Skerrow. 1989. Changes to desmosomal antigens and lectin-binding sites during differentiation in normal human epidermis: a quantitative ultrastructural study. *J. Cell Sci.* 92:667–677.

Smith, F.J., A.D. Irvine, A. Terron-Kwiatkowski, A. Sandilands, L.E. Campbell, Y. Zhao, H. Liao, A.T. Evans, D.R. Goudie, S. Lewis-Jones, et al. 2006. Loss-of-function mutations in the gene encoding filaggrin cause ichthyosis vulgaris. *Nat. Genet.* 38:337–342.

Steinert, P.M., and L.N. Marekov. 1999. Initiation of assembly of the cell envelope barrier structure of stratified squamous epithelia. *Mol. Biol. Cell.* 10:4247–4261.

Sur, I., B. Rozell, V. Jaks, A. Bergström, and R. Toftgård. 2006. Epidermal and craniofacial defects in mice overexpressing Klf5 in the basal layer of the epidermis. *J. Cell Sci.* 119:3593–3601.

Toomes, C., J. James, A.J. Wood, C.L. Wu, D. McCormick, N. Lench, C. Hewitt, L. Moynihan, E. Roberts, C.G. Woods, et al. 1999. Loss-of-function mutations in the cathepsin C gene result in periodontal disease and palmoplantar keratosis. *Nat. Genet.* 23:421–424.

Yamasaki, K., J. Schauber, A. Coda, H. Lin, R.A. Dorschner, N.M. Schechter, C. Bonnart, P. Descargues, A. Hovnanian, and R.L. Gallo. 2006. Kallikrein-mediated proteolysis regulates the antimicrobial effects of cathelicidins in skin. *FASEB J.* 20:2068–2080.

Yang, T., D. Liang, P.J. Koch, D. Hohl, F. Kheradmand, and P.A. Overbeek. 2004. Epidermal detachment, desmosomal dissociation, and destabilization of corneodesmosin in Spink5−/− mice. *Genes Dev.* 18:2354–2358.

Zeeuwen, P.L. 2004. Epidermal differentiation: the role of proteases and their inhibitors. *Eur. J. Cell Biol.* 83:761–773.